CHEMISTRY
A EUROPEAN JOURNAL

ChemPubSoc
Europe

DOI: 10.1002/chem.201202391

Guest Covalent Capture by a Host: A Biomimetic Strategy for the Selective Functionalization of a Cavity

Nicolas Menard, Olivia Reinaud, and Benoit Colasson*[a]

Abstract: A biomimetic strategy for the monofunctionalization of a calix[6]-arene core is described. It is based on host–guest chemistry (mimicking the Michaelis–Menten adduct in enzymes) and allows the finely tuned pre-organization of the substrate (an alkyne) with respect to the reactant (three azido groups introduced at the calixarene large rim). It is shown that the thermal Huisgen reaction implemented in this work proceeds under very mild conditions with total regioselectivity of the cycloaddition process. The scope of the reaction was explored and the results suggest that such a supramolecular strategy is quite versatile and could be applied to the selective functionalization of other cavitands bearing different recognition patterns. A detailed structural, thermodynamic, and kinetic study is also reported, highlighting interesting biomimetic features: The importance of the host–guest adduct strength, the high sensitivity of the reaction to the pre-organization of the reactive partners (alkyne vs. azide), and a significant impact of the embedment on the transition state. The self-coordination of the monofunctionalized products was also studied and an "*endo*/*exo*" switch of the internal side-chain could be triggered by adding competitive ligands.

Keywords: biomimetics · calixarenes · host–guest systems · regioselectivity · zinc

Introduction

Selective desymmetrization is a classic challenge in organic synthesis. The selective transformation of one functional group among other identical groups is a difficult task and often mixtures are generated.[1] Consequently, the desired desymmetrized molecule is obtained in low-to-moderate yield. The synthesis and purification of larger desymmetrized molecules may be even more tedious. Nevertheless, the need for such structures is often required when one wants to introduce different reactive functionalities, add cooperativity, or explore multivalency in host–guest systems.[2] Highly symmetrical parent macrocycles such as resorcinarenes,[3] cucurbiturils,[4] cyclodextrins,[5] and calix[*n*]arenes[6] are often encountered in supramolecular chemistry as molecular scaffolds for hosts, sensors, or catalysts. Reliable and useful synthetic procedures allowing for the selective transformation of one and only one reactive site of these macromolecules are scarce. The monofunctionalization of cyclodextrins is often achieved in low-to-moderate yield because of the need for chromatographic separation.[7] Very recently, one procedure based on the covalent capture strategy proved to be more selective.[8] Only a few procedures for the monofunctionalization of cucurbiturils are available.[9] As far as resorcinarene receptors are concerned, the modification of one wall out of four has been developed and extensively used by Rebek and co-workers.[10]

Synthetic procedures for the monofunctionalization of calix[6]arene macrocycles are rare. We previously reported a unique method for the selective monofunctionalization of a tris-azidocalix[6]arene[11] through a combination of the thermal Huisgen cycloaddition of azido compounds to acetylenes[12] and the host–guest properties of Zn^{II}–calix[6]arene-based funnel complexes.[13] 4-Pentyn-1-amine ($(C_3)NH_2$) can coordinate to the Zn^{II} ion, placing the acetylene in close vicinity to the three azido groups, thus pre-organizing the reactants. The cycloaddition occurs upon heating the complex to give the monofunctionalized complex $[ZnM_{(C_3)NH_2}]^{2+}$ (Scheme 1).[14] Subsequent cycloaddition reactions are prevented for two reasons: 1) Under such conditions, the intermolecular cycloaddition reaction is much slower as it requires much more drastic conditions (higher temperature and concentrations) and 2) the cavity of the calixarene is now occupied, preventing a second molecule of 4-pentyn-1-amine from displacing the now covalently linked amino chain and reacting intramolecularly.[15] This reaction is 100% selective towards monofunctionalization and creates exclusively the 1,5-triazole regioisomer.[11]

In this example, the "monoclick" reaction occurs because of the geometric fit between the acetylene and the azido groups. We intended to explore the scope of this methodology. To do so, we studied a variety of substrates that can be used to monofunctionalize the calixarene precursor. The acetylene guest can be constructed from three modifiable

[a] Dr. N. Menard, Prof. Dr. O. Reinaud, Dr. B. Colasson
Laboratoire de Chimie et Biochimie Pharmacologiques et Toxicologiques, CNRS UMR 8601
Université Paris Descartes, PRES Sorbonne Paris Cité
45 rue des Saints Pères, 75006 Paris (France)
Fax: (+33) 142-868-387
E-mail: benoit.colasson@parisdescartes.fr

Supporting information for this article is available on the WWW under http://dx.doi.org/10.1002/chem.201202391.

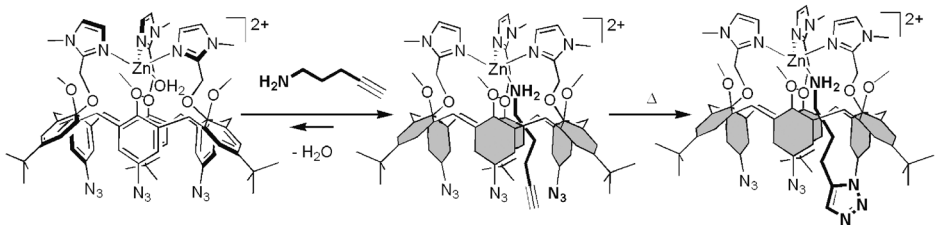

Scheme 1. Reaction pathway for the monoclick reaction with 4-pentyn-1-amine (the structures of the complexes have been simplified for clarity).

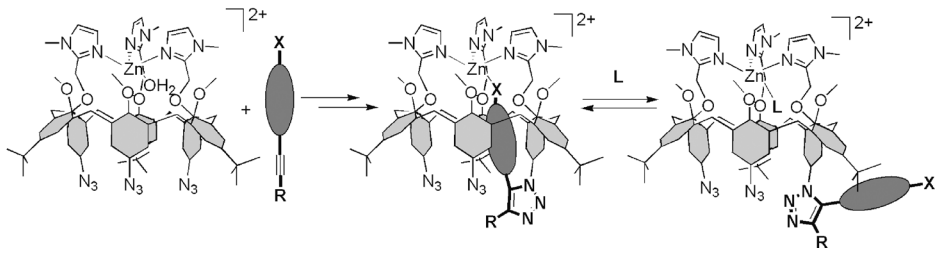

Scheme 2. Schematic representation of the monoclick reaction with a reactive guest bearing a coordinating function X, a spacer, the reactive acetylenic group, and a substituent R. The coordinating chain of the monofunctionalized complex can be either *endo* or *exo* with respect to the cavity, depending on the nature of X, R, the spacer, and the nature of the competitive ligand L.

parts: The coordinating group X (primary amine, alcohol), a spacer that can vary in length and in shape between X and the reactive acetylene function, and finally a terminal functionality R that can vary in size or in electronic properties (Scheme 2). We then investigated the relationship between the thermodynamically controlled complexation step and the kinetics of the cycloaddition step.

The monoclick reaction of such a guest provides a novel calix[6]arene-based ligand M_{CnX} (Scheme 2), which differs from classical "funnel complexes" as an additional coordinating group X is covalently linked to the large rim of the calixarene. Such a system is prone to undergo self-coordination and offers an interesting example of an "ouroboros-like" molecule as defined by Durola and Rebek.[16] Hence, in addition to methodological studies yielding these monofunctionalized calixarene complexes, we wish to describe and discuss their specific host–guest properties. In this respect, we have studied the structural and conformational changes accompanying self-coordination and the factors controlling the intramolecular coordination to the zinc cation, that is, the "*endo*/*exo*" equilibrium of the internal coordinating arm.

Results and Discussion

First, we evaluated the scope of the reaction by using primary amine ligands, which are the best guests for Zn–calixarene funnel complexes. The strong association to the zinc metal center provides unambiguous characterization of the intermediates and final compounds and facilitates discussion about the factors controlling reaction efficiency and structural modifications. In the second part, this synthetic methodology has been applied to alcohols. The differences and similarities between the reactions with the amines and alcohols will be emphasized. In particular, the thermodynamics of the intramolecular coordination of the hydroxy arm will be discussed.

Monoclick reactions with primary amines:

Effect of spacer length: The spatial proximity of the acetylene and the three azido groups appears to be one of the keys to monofunctionalization. The rate of reaction should be enhanced if the acetylene of the coordinated guest faces precisely the azido groups present on the large rim. Thus, we anticipated the existence of an optimal length for the spacer. To optimize our system, we studied three different alkylamines that differ only in the number n of methylene groups in the spacer: $HC{\equiv}C(CH_2)_nNH_2$ ($n=3$, 4, and 5): 4-Pentyn-1-amine ($(C_3)NH_2$), 5-hexyn-1-amine ($(C_4)NH_2$), and 6-heptyn-1-amine ($(C_5)NH_2$).

Synthesis and characterization of the three monoclick complexes: The three pre-click host–guest adducts HG_n were synthesized in situ from $[ZnX_6N_3](ClO_4)_2$ and the corresponding amines (see Figure 1) and characterized by ^1H NMR spectroscopy (see Figure 2A, C, and E) in CD_3CN. All the ^1H NMR spectra exhibit the same pattern and chemical shifts except for the resonances in the high-field region, which attests to the coordination of the amine to the metal center and its encapsulation in the cavity of the complex. The monoclick reactions were conducted in toluene at reflux with two equivalents of amine to provide the corresponding monofunctionalized Zn^{II} complexes in high yields (95, 93, and 92% for $[ZnM_{(C_3)NH_2}](ClO_4)_2$, $[ZnM_{(C_4)NH_2}](ClO_4)_2$, and $[ZnM_{(C_5)NH_2}](ClO_4)_2$, respectively). The reactions were completed within 2 hours for $n=3$ and 4, and 5 hours for $n=5$. The products were isolated by precipitation with Et_2O and centrifugation or filtration, depending on the scale of the reaction.

The products were all characterized by positive electrospray mass spectroscopy (EIMS) after demetalation of the samples by addition of trifluoroacetic acid (TFA). In all cases, a single peak was observed corresponding to the protonated monofunctionalized ligands $[M_{C_nNH_2}+H]^+$. Neither the bis- nor tris-adduct was ever observed, which proves that the monofunctionalization reaction is extremely selective in all three cases. The products were characterized by

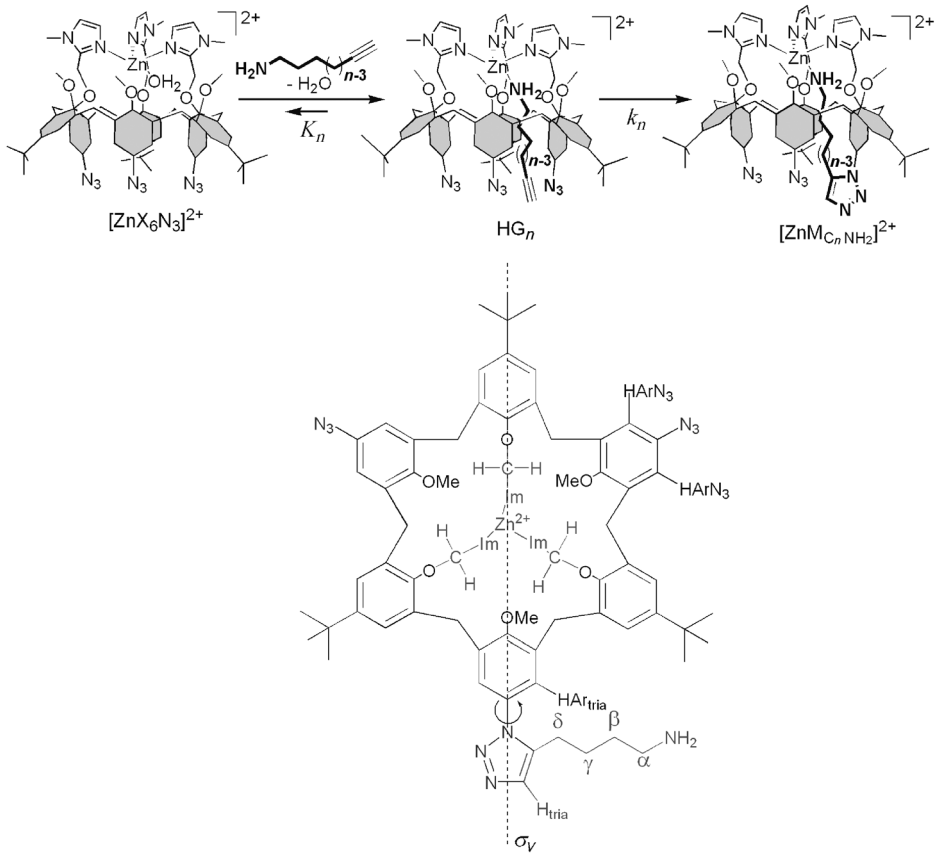

Figure 1. Top: Reaction pathway for the monoclick reactions of 4-pentyn-1-amine ($n=3$), 5-hexyn-1-amine ($n=4$), and 6-heptyn-1-amine ($n=5$). The corresponding complexation constant and the rate constant of the intramolecular cycloaddition are denoted as K_n and k_n, respectively. Bottom: Representation of the planar projection of the monofunctionalized complex $[ZnM_{(C_4)NH_2}]^{2+}$ emphasizing the vertical symmetry plane σ_v. For clarity, the bond between the amino group and the Zn^{II} ion is not represented and the alkyl chain is represented out of the symmetry plane.

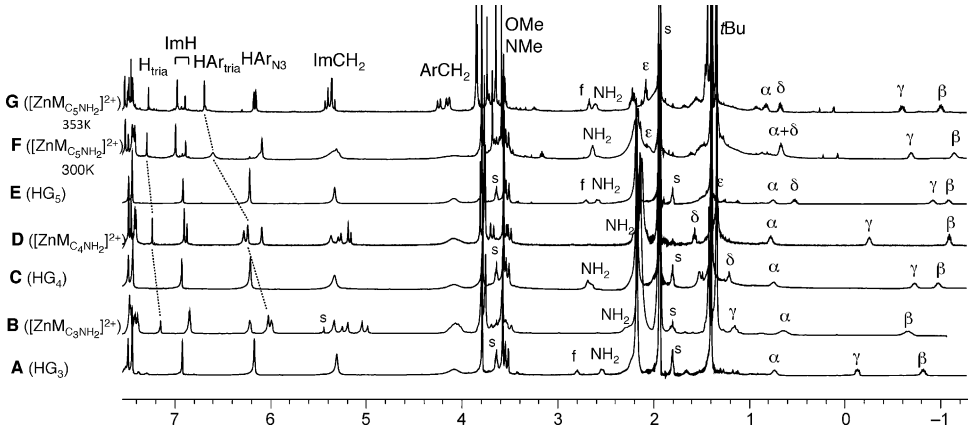

Figure 2. ^{1}H NMR spectra in CD_3CN of inclusion complexes HG_n and the corresponding monofunctionalized complexes $[ZnM_{CnNH2}]^{2+}$ ($n=3$, 4, 5): A) HG_3 (500 MHz, 300 K), B) $[ZnM_{(C_3)NH_2}]^{2+}$ (250 MHz, 300 K), C) HG_4 (500 MHz, 300 K), D) $[ZnM_{(C_4)NH_2}]^{2+}$ (500 MHz, 300 K), E) HG_5 (500 MHz, 300 K), F) $[ZnM_{(C_5)NH_2}]^{2+}$ (500 MHz, 300 K), and G) $[ZnM_{(C_5)NH_2}]^{2+}$ (500 MHz, 353 K) (f: free amino-acetylene; s: residual solvent; the methylene groups of the alkyl chain are denoted as α, β, γ, δ, and ε, starting from the NH_2 group).

^{1}H NMR spectroscopy (Figure 2B, D, and G), evidencing further the high selectivity of the reaction. A new singlet in the aromatic region attested to the formation of the triazole moiety. New upfield resonances appeared; the integration of these resonances indicates a guest/calixarene ratio of 1:1, which is consistent with a monofunctionalized calixarene in which the amino chain is coordinated to the Zn^{II} ion through the cavity. The resonances of the monofunctionalized complexes $[ZnM_{(C_3)NH_2}]^{2+}$ and $[ZnM_{(C_4)NH_2}]^{2+}$ are sharp at 300 K, whereas the resonances of the monofunctionalized complex $[ZnM_{(C_5)NH_2}]^{2+}$, especially the resonances of the imidazole arms $ImCH_2$, are broad at 300 K. However, at 353 K, the resonances sharpen. This indicates that $[ZnM_{(C_5)NH_2}]^{2+}$ has a restricted conformational mobility at 300 K that is slow on the NMR timescale. Because this phenomenon was not observed for $[ZnM_{(C_3)NH_2}]^{2+}$ or $[ZnM_{(C_4)NH_2}]^{2+}$, we can conclude that the longer alkyl chain imposes some distortion on the calixarene that hinders its conformational mobility (see below). In comparison with the pre-click inclusion complexes, the ^{1}H NMR spectra display a higher number of signals, consistent with a symmetry decrease from C_{3v} to C_s (Figure 1). Although the $ImCH_2$ protons resonate as a singlet in the inclusion complexes, after reaction they split into three signals: One singlet and two doublets experiencing a ^2J coupling. This is consistent with the existence of a σ_v symmetry plane, which differentiates the $ImCH_2$ that belongs to the σ_v plane (one singlet integrating for 2H) and two pairs of protons (two doublets integrating for 4H). Likewise, the initial HAr_{N3} signal is a singlet. After desymmetrization, the six protons are differentiated into three singlets integrating for two protons each: One singlet for HAr_{tria} and two singlets for the remaining HAr_{N3}. The

initial *t*Bu singlet is also split into two singlets integrating for 9H (for the *t*Bu that belongs to the symmetry plane) and 18H (for the two *t*Bu on either side of the symmetry plane). In the same manner, the methoxy groups (OCH_3) are split from one singlet (9H) into two singlets integrating for 3H and 6H, respectively. This split is a general trend for all the other groups of protons (NCH_3, ImH) for which one set of protons belongs to the symmetry plane and the other two sets are on each side of the plane.

Optimization of the chain length: All three monofunctionalized complexes were obtained in high yields after reaction for 2 hours for $(C_3)NH_2$ and $(C_4)NH_2$, and 5 hours for $(C_5)NH_2$. We wondered what was the impact of the length of the spacer on the kinetics of the reaction. To answer this question, two competitive monoclick reactions were carried out: $(C_3)NH_2$ versus $(C_4)NH_2$ and $(C_4)NH_2$ versus $(C_5)NH_2$. The monoclick reaction is a two-step process: Inclusion of the amino guest followed by intramolecular Huisgen cycloaddition. To fully understand the origin of the anticipated difference in the reaction rates, the thermodynamic and kinetic parameters of these two steps were analyzed (see Figure 1 for the definition of the parameters K_n and k_n).

The competitive complexation studies were carried out in CD_3CN at 300 K. A known mixture of 4-pentyn-1-amine ($n=3$) and 5-hexyn-1-amine ($n=4$) was added to a solution of precursor complex $[ZnX_6N_3]^{2+}$ in CD_3CN to yield quantitatively a mixture of inclusion complexes HG_3 and HG_4 (Figure 3C), identified by comparison with the pure inclusion complexes (Figure 3A and B). Relative integration of the upfield resonances of the coordinated guests provided the relative ratio of the inclusion complexes, which, corrected by the ratio of the free amines, provided the ratio of the binding constants: $K_4/K_3=(1.81\pm0.20)$.[17] A similar competition experiment was conducted with $(C_4)NH_2$ and $(C_5)NH_2$, which provided the ratio $K_4/K_5=(1.87\pm0.20)$ (for more details, see the Supporting Information). Therefore $(C_4)NH_2$ is the best amino-acetylene ligand of all three for inclusion. The formation of the host–guest complexes is enthalpically driven by the formation of a bond between NH_2 and the metal center.[18] The moderate selectivity of the host complex for $(C_4)NH_2$ is probably controlled by secondary CH–π interactions between the methylene groups and the calixarene cavity.

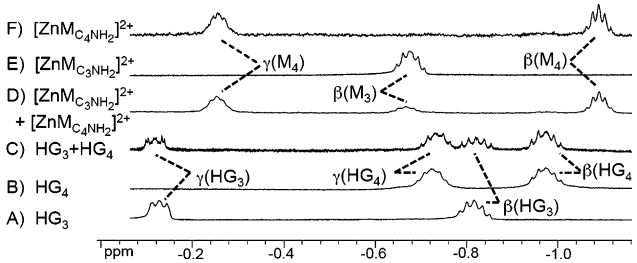

Figure 3. ^1H NMR (CD_3CN, 500 MHz, 300 K) spectra in the high-field region. From bottom to top: A) HG_3, B) HG_4, C) HG_4+HG_3 with 10 equiv of a 1:1 mixture of $(C_3)NH_2/(C_4)NH_2$, D) $[ZnM_{(C_3)NH_2}]^{2+}+[ZnM_{(C_4)NH_2}]^{2+}$ after heating of mixture C in toluene at 110°C, E) $[ZnM_{(C_3)NH_2}]^{2+}$, and F) $[ZnM_{(C_4)NH_2}]^{2+}$. The resonances of the β- and γ-methylene groups of the coordinated alkyl chain are indicated.

We then studied how the difference in the pre-organization of the host–guest inclusion complexes HG_n influences the rate of the cycloaddition reaction by means of competitive monoclick reactions. A known mixture of host–guest inclusion complexes HG_3 and HG_4 and a large excess of the corresponding amines in toluene were heated at 110°C for 2 hours and, after isolation, the resulting mixture of monofunctionalized calixarenes $[ZnM_{(C_3)NH_2}]^{2+}$ and $[ZnM_{(C_4)NH_2}]^{2+}$ was analyzed by ^1H NMR spectroscopy in CD_3CN (Figure 3D–F). The kinetic law for each intramolecular reaction is given by Equation (1).

$$v_n = k_n[HG_n] = k_nK_n[C_nNH_2][ZnX_6N_3]/[H_2O] \quad (1)$$

During the reaction, the ratio $[(C_3)NH_2]/[(C_4)NH_2]$ varies little and thus can be considered as a constant. Hence, we can write Equation (2).

$$v_4/v_3 = [ZnM_{(C_4)NH_2}]_\infty/[ZnM_{(C_3)NH_2}]_\infty = k_4[HG_4]_0/k_3[HG_3]_0 \quad (2)$$

From this we calculate Equation (3) (for more details, see the Supporting Information).

$$k_4/k_3 = ([ZnM_{(C_4)NH_2}]_\infty/[ZnM_{(C_3)NH_2}]_\infty)([HG_3]_0/[HG_4]_0) = (1.25\pm0.10) \quad (3)$$

A similar experiment was conducted with amines $(C_4)NH_2$ and $(C_5)NH_2$, which provided $k_4/k_5=(2.28\pm0.20)$.

Therefore, the highest rate constant for the intramolecular cycloaddition was reached with 5-hexyn-1-amine, which indicates that the geometry of the corresponding host–guest complex HG_4 is the closest to the transition state. In this case, the acetylene faces best the three azido groups. The effect is more significant when $(C_4)NH_2$ is compared with the longest chain $(C_5)NH_2$.

The trends in the values of the rate constants and the complexation constants follow the same pattern. Hence, the best ligand leads coincidentally to the highest reaction rate. 5-Hexyn-1-amine is unambiguously the best substrate for this monoclick reaction due to the synergy between the two phenomena. The synergy between thermodynamics and kinetics is often at work in enzymatic systems. It can be quantified in the Michaelis–Menten model by the ratio k_{cat}/K_M, k_{cat} being the turnover number and K_M the Michaelis constant. When the assumption of a rapid equilibrium is fulfilled, K_M is equal to the dissociation constant of the enzyme–substrate complex.[19] In the system presented herein, the ratio k_{cat}/K_M is equivalent to k_nK_n. Calculation gives $k_4K_4/k_3K_3=2.2$ and $k_4K_4/k_5K_5=4.3$. The highest value for k_4K_4 indicates a better specificity of the transformation of the tris-azido–calixarene complex with the $(C_4)NH_2$ substrate. Ac-

Table 1. Chemical shifts (CD_3CN, 500 MHz, 300 K[a]) of species investigated in this study.[b]

						δ [ppm]					
	α	β	γ	δ	ε	*t*Bu	OCH_3	NCH_3	$ImCH_2$	HArN	ImH
$[ZnX_6N_3]^{2+}$						1.38	3.65	3.65	5.04	5.91	6.88
$(C_3)NH_2$	2.79	1.64	2.24								
HG_3	0.74	−0.82	−0.13			1.40	3.58	3.79	5.31	6.17	6.93
CIS_3	−2.05	−2.46	−2.37			0.02	−0.07	0.14	0.27	0.26	0.05
$[ZnM_{(C_3)NH_2}]^{2+}$	0.64	−0.66	1.15			1.43 (9H)	3.80 (3H)	3.80 (3H)	5.34 (s)	6.00 (N_3)	6.84 (1H)
						1.34 (18H)	3.58 (6H)	3.76 (6H)	5.02 (d1)	6.22 (N_3)	6.85 (2H)
									5.23 (d2)	6.03 (tria)	
$\Delta\delta_3$	−0.10	0.16	1.28			0.03 (9H)	0.22 (3H)	0.01 (3H)	0.03 (s)	−0.17 (N_3)	−0.09 (1H)
						−0.06 (18H)	0.00 (6H)	-0.03 (6H)	−0.29 (d1)	0.05 (N_3)	−0.08 (2H)
									−0.08 (d2)	−0.14 (tria)	
$(C_4)NH_2$	2.7	1.55	1.55	2.2							
HG_4	0.75	−0.97	−0.73	1.22		1.39	3.57	3.79	5.34	6.21	6.93
CIS_4	−1.95	−2.52	−2.28	−0.98		0.01	−0.08	0.14	0.30	0.30	0.05
$[ZnM_{(C_4)NH_2}]^{2+}$	0.78	−1.09	−0.25	1.57		1.41 (9H)	3.76 (3H)	3.81 (3H)	5.37 (s)	6.10 (N_3)	6.87 (1H)
						1.34 (18H)	3.57 (6H)	3.77 (6H)	5.18 (d1)	6.24 (N_3)	6.90 (2H)
									5.28 (d2)	6.28 (tria)	
$\Delta\delta_4$	0.03	−0.12	0.48	0.35		0.02 (9H)	0.19 (3H)	0.02 (3H)	0.03 (s)	−0.11 (N_3)	−0.06 (1H)
						−0.05 (18H)	0.00 (6H)	−0.02 (6H)	−0.16 (d1)	0.03 (N_3)	−0.03 (2H)
									−0.06 (d2)	0.07 (tria)	
$(C_5)NH_2$	2.71	1.55	1.55	1.55	2.17						
HG_5	0.75	−1.08	−0.92	0.52	1.80	1.40	3.56	3.80	5.34	6.22	6.92
CIS_5	−1.96	−2.63	−2.47	−1.03	−0.37	0.02	−0.09	0.15	0.30	0.31	0.04
$[ZnM_{(C_5)NH_2}]^{2+}$	0.70	−1.11	−0.66	0.70	2.09	1.42 (9H)	3.71 (3H)	3.82 (3H)	5.37[a] (s)	6.16[a] (N_3)	6.92 (1H)
						1.38 (18H)	3.62 (6H)	3.83 (6H)	5.35[a] (d1)	6.18[a] (N_3)	7.02 (2H)
									5.42[a] (d2)	6.70[a] (tria)	
$\Delta\delta_5$	−0.05	−0.03	0.26	0.18	0.29	0.02 (9H)	0.15 (3H)	0.02 (3H)			0.00 (1H)
						−0.02 (18H)	0.06 (6H)	0.03 (6H)			0.10 (2H)

[a] With the exception of the peaks corresponding to CH_2Im, HAr_{N3}, and HAr_{tria} of $[ZnM_{(C_5)NH_2}]^{2+}$, which are broad at 300 K and were recorded at 353 K. [b] First row is precursor complex $[ZnX_6N_3]^{2+}$. Each of the other three rows ($n=3, 4, 5$) is divided into five sub-rows: A) Free amine ($n=3, 4, 5$); B) HG_n ($n=3, 4, 5$); C) CIS (difference between $\delta_{FreeAmine}$ in and out, or for the calixarene: difference between $HG_{n=3,4,5}$ and the initial complex; D) Monofunctionalized complex $[ZnM_{CnNH2}]^{2+}$ ($n=3, 4, 5$); E) $\Delta\delta_n$ (difference between the chemical shifts of the monofunctionalized complexes $[ZnM_{CnNH2}]^{2+}$ and the corresponding inclusion complex HG_n. The methylene groups of the alkyl chain are denoted as α, β, γ, δ, and ε, starting from the NH_2 group).

cordingly, $n=4$ corresponds to the optimized length for the spacer.

Origin of the observed specificity based on a conformational analysis: As pre-organization is key for this reaction, we studied the host–guest symmetry changes and the adaptation process that both the calixarene host and the guest alkyl chain must undergo to yield the monofunctionalized complex. To this end we analyzed the conformations of both the inclusion complexes and the monofunctionalized complexes in CD_3CN (see Figure 2 and Table 1).

1) Conformational comparison of the inclusion complexes HG_n: In all cases, the aromatic walls of the calixarene cavity shield the amino guest upon complexation and lead to an upfield shift of the resonances of the alkyl chain.[13a,20] We defined the complex-induced shift (CIS) value as the difference between the chemical shifts of a group of protons in the inclusion complex HG_n and in the free ligand. The CIS values are reported in Table 1. In all cases, H_β has the greatest CIS value, which means that it is the most shielded. Nevertheless, from one guest to another, the difference in CIS is 0.05 ppm at most, which indicates that the shielding effects are very similar. Therefore all three guests are positioned at the same height inside the calixarene cavity. Upon inclusion of the guests, some resonances of the calixarene unit remain almost unchanged. For instance, there is little effect of the guest complexation on the *t*Bu (ca. 0.01 ppm) or ImH CIS (ca. 0.04 ppm). However, the resonances of $ImCH_2$ are different to those of the precursor complex, but are almost identical for the three amino guests (CIS $\approx$0.28 ppm). The same is true for methoxy groups (CIS ≈ -0.08 ppm) and HAr_{N3} (CIS $\approx$0.28 ppm). These data highlight a slight change in the conformation of the calixarene upon complexation of the guests. However, for all three, the conformational change is almost identical, which suggests that the difference in the reactivities of the three amino-alkynes does not come from the distortion of the calixarene at the complexation step.
2) Conformational analysis of the monoclick products $[ZnM_{CnNH2}]^{2+}$: Unlike the inclusion complexes, there are clear differences between the spectra of the monoclick products, which indicates that the three products have

significantly different conformations (Figure 2). These differences can be observed by measuring the differences between the chemical shifts of the monoclick product and the corresponding inclusion complex ($\Delta\delta_n$). To picture completely the influence of the chain length on the structural properties, two conformational features need to be discussed: Distortion of the calixarene cone and restricted conformational mobility.

Distortion of the calixarene cone: After the click reaction, the Ar*t*Bu units are differentiated but in all three cases the $\Delta\delta$ values are very close to zero for all complexes. Therefore the Ar*t*Bu units see little conformational change following the cycloaddition step, which is consistent with the fact that these aromatic units are projected away from the calixarene cavity and are little affected by modifications to the inside of the cavity (Figure 4). The aromatic unit that sees the

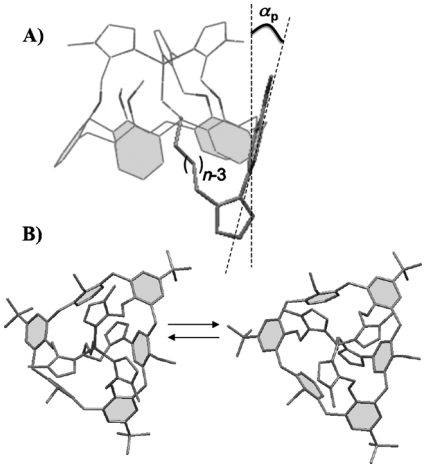

Figure 4. Schematic representations of A) the pivot of the Ar_{tria} unit by an α_p angle (side-view, the *t*Bu and N_3 groups have been omitted for clarity) and B) the equilibrium of the helix inversion around the metal center and the distortion of the calixarene structure (top view, the N_3 groups have been omitted for clarity).

greatest environmental change is the Ar_{tria} unit because it becomes covalently linked to the coordinated amino chain. In all three cases, the $\Delta\delta_n$ value for its methoxy group (Table 1, column OCH_3 (3H)) is positive. This indicates that the methoxy groups are pushed away from the cavity forcing the Ar_{tria} unit to pivot towards the inside of the shielding cavity (Figure 4A). Interestingly, $\Delta\delta_n$ for the methoxy group increases as the alkyl chain becomes shorter (0.15, 0.19, and 0.22 ppm for $n=5$, 4, and 3, respectively), which indicates that with a shorter chain, the aromatic unit pivots more towards the inside of the cavity. Although the signs of the $\Delta\delta_n$ values for HAr_{tria} can hardly be interpreted in terms of conformational change because the chemical transformation of azido to triazole has a great influence on the chemical shifts, their relative values can be compared. The $\Delta\delta_n$ values for HAr_{tria} (0.48, 0.07, and −0.14 ppm for $n=5$, 4, and 3, respectively) and the H_{tria} chemical shifts (7.33, 7.24, and 7.15 ppm for $n=5$, 4, and 3, respectively) decrease significantly when the spacer is shorter, which also indicates that the Ar_{tria} aromatic unit rotates more towards the inside of the cavity when the chain is shorter.

The rotation of the two remaining Ar_{N3} units can be measured by the average chemical shift of their aromatic protons HAr_{N3}. In all cases, the Ar_{N3} units are in very similar positions (the average chemical shift for the HAr_{N3} protons is 6.11 ppm for $[ZnM_{(C_3)NH_2}]^{2+}$ and 6.17 ppm for both $[ZnM_{(C_4)NH_2}]^{2+}$ and $[ZnM_{(C_5)NH_2}]^{2+}$). Therefore there is no significant impact of the length of the spacer on the pivot of the remaining Ar_{N3} units.

The symmetry decrease from C_{3v} to C_s gives rise to newly differentiated protons that no longer resonate at the same frequency because they perceive different environments. The difference in the chemical shifts of protons that are no longer equivalent is an indication of the difference in the environment of these protons. Therefore a greater splitting in the ^1H NMR spectrum is indicative of a greater distortion of the calixarene cone. The splitting between the two sets of methoxy groups is greater when the chain is shorter (0.09, 0.19, and 0.22 ppm for $n=5$, 4, and 3, respectively). This phenomenon can also be observed for the two HAr_{N3} signals (0.02, 0.14, and 0.22 ppm for $n=5$, 4, and 3, respectively), the two $ImCH_2$ doublets (0.07, 0.10, and 0.21 ppm for $n=5$, 4, and 3, respectively), and, to a lesser extent, the two *t*Bu signals (0.04, 0.07, and 0.09 ppm for $n=5$, 4, and 3, respectively). Therefore shorter chains accentuate the distortion of the cone of the calixarene.

Resonance broadening and restricted conformational mobility: With $n=5$ only, a new phenomenon occurs: At 300 K, the resonances of $ImCH_2$, HAr_{tria}, and HAr_{N3} of $[ZnM_{(C_5)NH_2}]^{2+}$ are broad (Figure 2F) whereas they are sharp for $[ZnM_{(C_3)NH_2}]^{2+}$ and $[ZnM_{(C_4)NH_2}]^{2+}$ at the same temperature. In addition, the resonances of the $ArCH_{ax}$ protons, which are broad for $[ZnM_{(C_3)NH_2}]^{2+}$ and $[ZnM_{(C_4)NH_2}]^{2+}$, become even broader and can barely be seen in the spectrum (Figure 2F), which is indicative of a different conformational mobility of $[ZnM_{(C_5)NH_2}]^{2+}$. Indeed, at 353 K, all these resonances are sharper (Figure 2G). This reflects the fact that the longer chain imposes a constrained conformation on the calixarene structure and more precisely on the coordination arms (through the coordination of the amino group to the Zn^{II} ion) and the Ar_{tria} unit (through the triazole group). Thus, $[ZnM_{(C_5)NH_2}]^{2+}$ has a restricted conformational mobility that impacts on the helix inversion (see below).

Dynamics of the helix inversion at the metal center: We focused then on the influence of self-coordination on helix inversion, a conformational change experienced at the Zn^{II} cation coordination sphere (Figure 4B).[21] To study the dynamics of such a process, we conducted ^1H NMR experiments at various temperatures in CD_3CN and in $CDCl_3$, a noncoordinating solvent (see the Supporting Information).

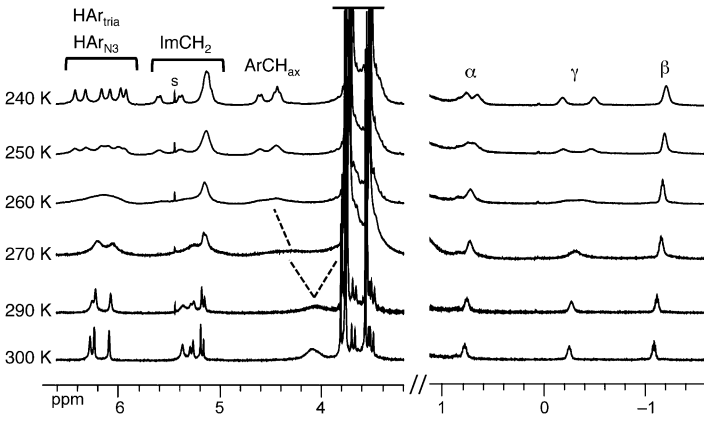

Figure 5. ^{1}H NMR spectra of monofunctionalized complex $[ZnM_{(C_4)NH_2}]^{2+}$ (CD_3CN, 500 MHz) at various temperatures (s: residual solvent).

The ^{1}H NMR spectrum of $[ZnM_{(C_4)NH_2}]^{2+}$ in CD_3CN (Figure 2D) is that of a C_s-symmetric species, which means that at 300 K the helicoidal inversion is fast on the NMR timescale. The loss of C_s symmetry in favor of the C_1-symmetric species can be observed when the solution is cooled to 240 K (Figure 5). Indeed, there are six signals for the six $[HAr_{N3}+HAr_{tria}]$ protons. There is also a clear splitting of the β- and γ-protons, which indicates that they have become diastereotopic. The $ImCH_2$ protons are divided into three AB systems. As previously observed for the tris-imidazole funnel complexes, the NMR data are consistent with the helicoidal structure of the coordination arms around the Zn^{II} ion.[21a] This helicoidal chirality is transferred to the whole calixarene structure that twists around its axis. In CD_3CN, the inversion barrier between the two helices is $\Delta G^{\neq}=(50.7\pm0.4)$ kJ mol^{-1} and was calculated for the $CH_2(\gamma)$ protons at their coalescence temperature ($T_c=(260\pm2)$ K). The spectrum of $[ZnM_{(C_5)NH_2}]^{2+}$ in CD_3CN is broad at 300 K (Figure 2F) and greatly resembles the spectrum of $[ZnM_{(C_4)NH_2}]^{2+}$ in CD_3CN at 280 K. This indicates that the helicoidal inversion is slower for $[ZnM_{(C_5)NH_2}]^{2+}$ than for $[ZnM_{(C_4)NH_2}]^{2+}$. Indeed, the inversion barrier between the two helices is $\Delta G^{\neq}=(54.9\pm0.4)$ kJ mol^{-1} for $[ZnM_{(C_5)NH_2}]^{2+}$ in CD_3CN (calculated for the $CH_2(\gamma)$ protons at their coalescence temperature $T_c=(265\pm2)$ K), which is greater than that for $[ZnM_{(C_4)NH_2}]^{2+}$. This result is also consistent with the competition study. In this case the spacer is too long so the chain is packed in the cavity and impacts on the mobility of the whole structure. Thus, the competition experiments are plainly corroborated by the conformational analysis of the monofunctionalized products by reasoning on a late transition state. A C_3 spacer is too short and imposes a distortion on the calixarene cone whereas a C_5 spacer is too long and imposes constrained conformations on the global structure. Both spacers compel energetically unfavorable constraints on their corresponding transition states, which explains their high energies relative to the optimal C_4 spacer.

In conclusion to this extensive conformational analysis, we have shown that the length of the spacer is a key element for the monoclick reaction. The optimal four-atom chain length ensures the best inclusion of the guest as well the highest reactivity of the host–substrate complex. In addition, the nature of the spacer has a great impact on the conformation of the monofunctionalized complex and on its conformational mobility.

Monofunctionalization with other amino guests: Having determined that the optimal length for the spacer is $n=4$, we decided to test other amino guests with four carbon atoms between the amino and the acetylene groups. The benzylamine-based guest ($ArCH_2NH_2$) presents a more rigid spacer. The other two substrates have the same aliphatic spacer as 5-hexyn-1-amine and the acetylene is substituted by *p*-methoxyphenyl (*p*MeOAr(C_4)NH_2) or *p*-nitrophenyl (*p*NO_2Ar(C_4)NH_2; Figure 6).

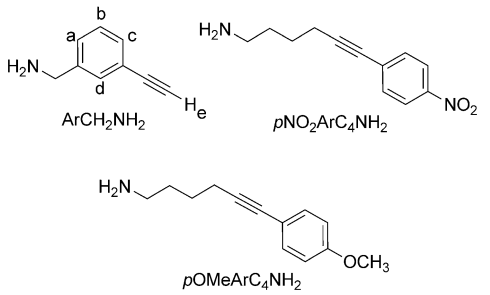

Figure 6. Aminoalkynes with a C_4 spacer.

Monofunctionalization with $ArCH_2NH_2$: The monoclick reaction proceeds in high yield with $ArCH_2NH_2$ (95%). The reaction is complete within 2 hours, like the corresponding aliphatic 5-hexyn-1-amine. The inclusion complex was obtained quantitatively by adding 1.1 equivalents of 3-ethynylbenzylamine to the $[ZnX_6N_3]^{2+}$ complex. The resonances of the guest protons are all shifted upfield, which is consistent with the inclusion of the guest in the cavity. The strongest shielding effects can be observed on H_a (CIS = −2.84 ppm) and H_d (CIS = −2.50 ppm), which is stronger than with an alkyl spacer (see Figure 7 for assignment). Protons H_b and H_c are also shielded, but to a lesser extent, which indicates that their positions are lower in the calixarene cavity. However, the CIS values for the calixarene protons are all very close to the CIS values for HG_4 (see the Supporting Information, Table 4.1), which means that the rigidity of the guest ligand does not have an impact on the conformation of the host–guest complex.

The ^{1}H NMR (CD_3CN, 500 MHz, 300 K) spectrum of $[ZnM_{ArCH_2NH_2}]^{2+}$ is consistent with a C_s-symmetrical complex. All the chemical shifts of the calixarene structure are similar to those of the $[ZnM_{(C_4)NH_2}]^{2+}$ complex. In this case, the signals from the $ArCH_{ax}$ protons are very sharp doublets, whereas they give broad resonances in $[ZnM_{(C_4)NH_2}]^{2+}$. This indicates that they waver in a more restricted space in $[ZnM_{ArCH_2NH_2}]^{2+}$. Consequently, we can conclude that

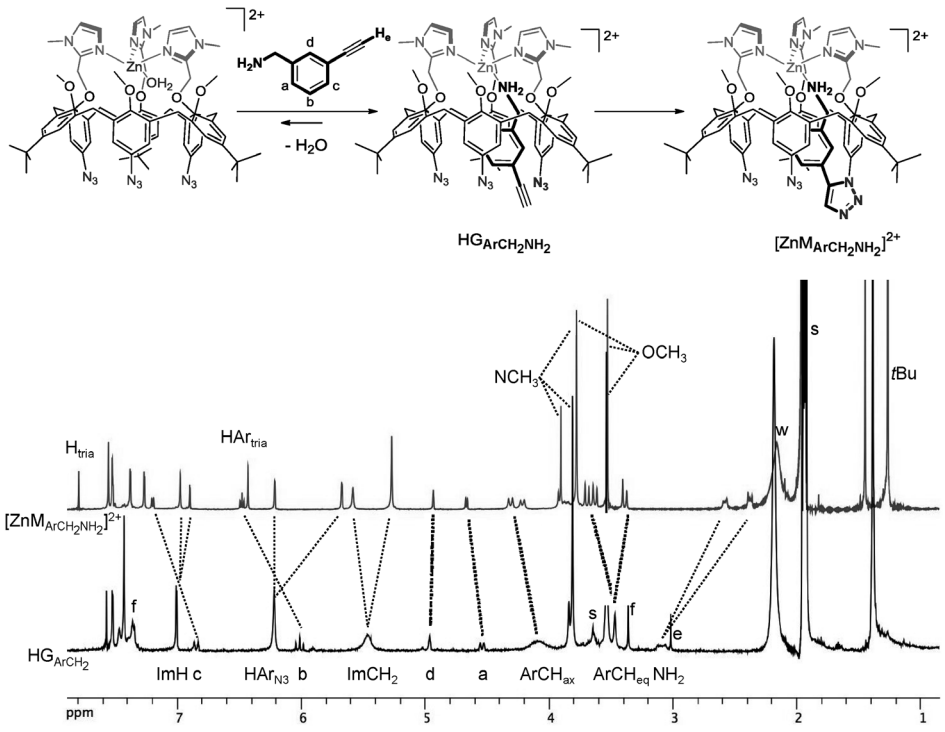

Figure 7. Top: Reaction pathway for the monoclick reaction with 3-ethynylbenzylamine. Bottom: ^{1}H NMR (CD_3CN, 500 MHz, 300 K) spectra of the inclusion complex $HG_{ArCH2NH2}$ and the monofunctionalized complex $[ZnM_{ArCH2NH2}]^{2+}$ (f: free ligand; s: residual solvent; w: water).

$[ZnM_{ArCH2NH2}]^{2+}$ is more rigid than $[ZnM_{(C_4)NH_2}]^{2+}$. The rigidity of the guest is then transferred to the monofunctionalized calixarene structure. ^{1}H NMR studies indicate that all six aromatic units are oriented very similarly to $[ZnM_{(C_4)NH_2}]^{2+}$ but the calixarene structure is much more distorted (see the Supporting Information for more details).

Monofunctionalization with substituted acetylenes: The monoclick reaction also proceeds in high yields with pNO$_2$Ar(C$_4$)NH$_2$ (91%) and pMeOAr(C$_4$)NH$_2$ (92%) substituted acetylenes but the reaction requires 5 hours to go to completion. This indicates that the substitution of the acetylene has a strong effect on the kinetics of the reaction.[22] This difference originates from a less favorable coordination step ($K_4/K_{pNO_2Ar(C_4)NH_2} = (1.60 \pm 0.20)$, see the Supporting Information for competition experiments) because of the bulky phenyl group in this position, as well as a less favorable intramolecular reaction ($k_4/k_{pNO_2Ar(C_4)NH_2} = (2.60 \pm 0.20)$). The discrimination based on host–guest adduct formation can be even more drastic: A bulkier group (anthracene) prevents the coordination of the amino guest and no conversion for the monoclick reaction is observed. In both cases the spacer is the same ($n = 4$) but the acetylene is differently functionalized. The chemical shifts of the monofunctionalized complexes are all very similar to the chemical shifts of $[ZnM_{(C_4)NH_2}]^{2+}$. This indicates that the three monofunctionalized complexes $[ZnM_{pOCH_3(C_4)NH_2}]^{2+}$, $[ZnM_{pNO_2Ar(C_4)NH_2}]^{2+}$, and $[ZnM_{(C_4)NH_2}]^{2+}$ have very similar conformations. Therefore the nature of the spacer is what determines the conformation of the calixarene structure. The functionalization of the triazole at the 5-position has little impact on this structure.

Conclusions on the monoclick reactions with amine substrates: The monofunctionalized reaction developed with amine substrates is an easy, clean, and efficient method for selectively monofunctionalizing calix[6]arenes in high yields. We have established that there is an optimal length of four carbon atoms for the spacer, which originates from the synergy between the thermodynamically controlled complexation step and the kinetically controlled intramolecular cycloaddition step. For the same optimal length, different structures for the spacer and for the alkyne substituent can be used for the monoclick reaction provided they are not too bulky. The monoclick reaction works with different amines, despite distorting the calixarene structure. The distortion has a low energetic cost, which indicates that we are dealing with a very flexible cavity system. The conformation of the monofunctionalized calixarene is imposed by the nature of the spacer. The spacer has a steric limit because it should fit into the cavity and not differ too much from the optimum $n = 4$. There is also a steric limit for the group functionalizing the acetylene. Too much hindrance prevents coordination of the substrates and inhibits the intramolecular reaction.

Monoclick reactions with primary alcohols: Amines proved to be suitable for structural analysis because the intramolecular coordination is fully observed both in coordinating and noncoordinating solvents, thus avoiding a mixture of *endo* and *exo* isomers. Primary alcohols are weaker ligands than primary amines but their coordination to the Zn^{II} ion can still be observed in noncoordinating solvents.[14a] Starting with the conditions found for the amine substrates, the synthesis was optimized for the alcohols. This optimization is discussed below. The synthesis of a calixarene complex monofunctionalized by a hydroxy group enabled us to study the "*endo*/*exo*" dynamic equilibrium that operates under certain conditions.

Synthesis and characterization of the monoclick product $[ZnM_{(C_4)OH}]^{2+}$: 5-Hexyn-1-ol is the strict equivalent to 5-hexyn-1-amine as the only modified parameter is the coordinating group. Because water competes with the alcohol for

coordination at the metal center, the reaction was conducted in dry toluene at reflux. The optimized conditions required the use of ten equivalents of 5-hexyn-1-ol (vs. 2 equiv for 5-hexyn-1-amine) and 4 h of reflux (vs. 2 h for 5-hexyn-1-amine). Unlike with primary amines, the resulting monofunctionalized complex $[ZnM_{(C_4)OH}]^{2+}$ was generally isolated with some starting material $[ZnX_6N_3]^{2+}$ and a difunctionalized complex, which shows that the monoclick reaction with 5-hexyn-1-ol is less selective than with 5-hexyn-1-amine. After purification by column chromatography (during which decoordination of the metal cation occurred), pure monofunctionalized ligand $M_{(C_4)OH}$ was obtained. Upon recomplexation with $Zn(ClO_4)_2{\cdot}(H_2O)_6$ in CH_2Cl_2/CH_3CN, pure monofunctionalized calixarene $[ZnM_{(C_4)OH}]^{2+}$ was isolated in a yield of 70–95% (over two steps) depending on the run.

The monofunctionalized ligand $M_{(C_4)OH}$ was characterized by EIMS spectrometry (a single peak was observed at $m/z =$ 1350.7 for $[M_{C4OH}+H]^+$). The ^{1}H NMR spectrum of the ligand is broad in the usual solvents ($CDCl_3$, CD_3CN, [D_6]DMSO) at 300 K but the resonances are sharper at 360 K in [D_6]DMSO (Figure 8). The appearance of a singlet at 7.64 ppm (integrating for 1H) for H_{tria} on the newly formed triazole group, as well as the resonances for the one clicked alkyl chain attest to the monofunctionalization of the calixarene. In addition, the splitting of the *t*Bu, OCH_3, and $ImCH_2$ groups is consistent with a C_s-symmetrical species.

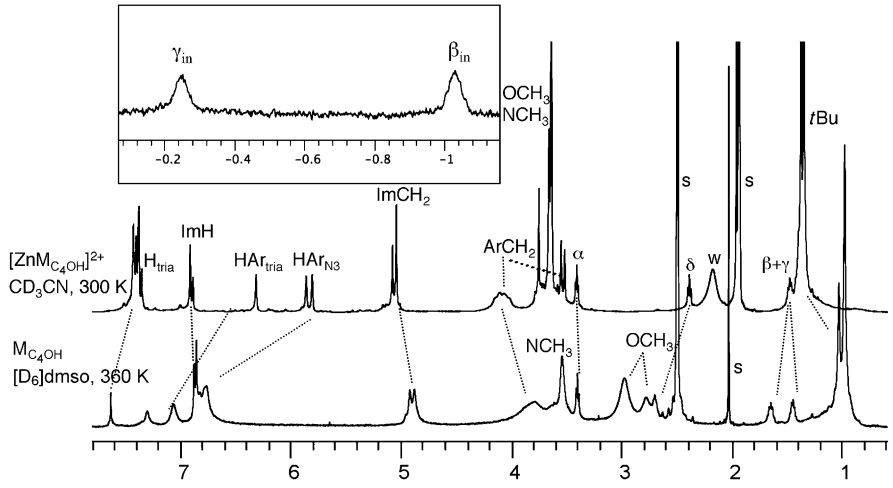

Figure 8. Bottom: ^{1}H NMR (500 MHz) spectrum of ligand M_{C4OH} ([D_6]DMSO, 360 K). Top: ^{1}H NMR (500 MHz) spectrum of complex $[ZnM_{C4OH}]^{2+}$ with zoom of the signals of the encapsulated β- and γ-methylene groups in the upfield region (CD_3CN, 300 K) (s: residual solvent; w: water).

The monofunctionalized complex $[ZnM_{(C_4)OH}]^{2+}$ was characterized by EIMS ($m/z = 1512.6$ for $[ZnM_{(C_4)OH}+ClO_4]^+$). The ^{1}H NMR spectrum in CD_3CN at 300 K displays sharp resonances and evidences one major product, consistent with a monofunctionalized calixarene (Figure 8). In contrast to $[ZnM_{(C_4)NH_2}]^{2+}$, the resonances of the alkyl chain in $[ZnM_{(C_4)OH}]^{2+}$ are not shielded. This indicates that the hydroxy group is not coordinated to the zinc cation and is displaced by one molecule of CD_3CN (*exo* situation for the chain). A second minor species can also be detected. Indeed, shielded resonances were also observed at −0.25 and −1.03 ppm, attesting to the existence of a self-coordinated complex (*endo* situation for the chain). At 300 K, the *exo* to *endo* ratio, evaluated by integration of the signals of the alkyl chain, is 93:7. This ratio was evaluated at different temperatures between 270 and 340 K (see the Supporting Information). Self-coordination of the hydroxy chain is favored at lower temperatures. The van't Hoff plot for the equilibrium of the displacement of the coordinated hydroxy chain by an acetonitrile molecule (*endo*/*exo* equilibrium) gave the following thermodynamic parameters: $\Delta_r H° = 11\ kJ\,mol^{-1}$ and $\Delta_r S° = 59\ J\,K^{-1}\,mol^{-1}$. The positive enthalpic change reflects the better affinity of the zinc cation for an alcohol compared with a nitrile.[13a] The favorable change in entropy can be rationalized by the expulsion of the alkyl chain outside of the cavity due to the decoordination and gain of conformational flexibility of both the chain and the calixarene core. In CD_3CN, the addition of one equivalent of a primary amine like propylamine yields quantitatively the inclusion complex $[ZnM_{(C_4)OH}(PrNH_2)]^{2+}$, which means that both the self-coordinated hydroxy chain and the acetonitrile molecule are displaced. This displacement is enthalpically driven by the strength of the Zn–N bond. The behavior of complex $[ZnM_{(C_4)OH}]^{2+}$ is very similar in CD_3OD because the two complexes (*endo* and *exo*) coexist at 300 K, the *exo* complex being largely favored (see the Supporting Information). In the noncoordinating solvent $CDCl_3$ at 325 K, the upfield resonances of the β- and γ-methylenes at −1.08 and −0.21 ppm, respectively, as well as the absence of resonances at 3.40 and 2.70 ppm for the α- and *δ*-methylenes, suggest the presence of only the self-coordinated complex. The only competing ligand in the media is residual water, which is not strong enough to displace the intramolecularly coordinated hydroxy chain.

Thus, the host–guest properties of the $[ZnM_{(C_4)OH}]^{2+}$ complex are very different to those of its amino analogue. The hydroxy chain can be chased out of the cavity by an exogenous alcohol, nitrile, or primary amine (Scheme 3). Nevertheless, compared with classic funnel complexes like $[ZnX_6tBu_6]^{2+}$, the affinity of $[ZnM_{(C_4)OH}]^{2+}$ for alcohols and nitriles is greatly reduced due to the control of the accessibility of the metal center by the self-coordination of the internal arm. In contrast, the amino-functionalized calixarene remains self-coordinated in all tested conditions.

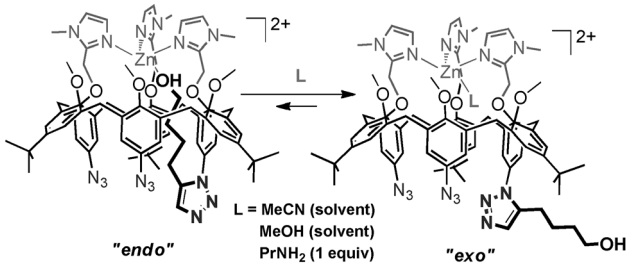

Scheme 3. Favorable displacement of the self-coordinated hydroxy chain of complex $[ZnM_{C4OH}](ClO_4)_2$ by coordinating solvents MeCN, MeOH, or $PrNH_2$ in stoichiometric proportions in any solvent.

Variable-temperature (VT) NMR experiments were conducted on $[ZnM_{(C_4)OH}]^{2+}$ in $CDCl_3$ (see the Supporting Information). The results are very similar to those obtained with $[ZnM_{(C_4)NH_2}]^{2+}$. Indeed, at 325 K, the spectrum of $[ZnM_{(C_4)OH}]^{2+}$ is characteristic of a C_s-symmetrical species in which the helicoidal inversion of the imidazole arms is fast on the NMR timescale. At 300 K, the signals broaden and at 266 K the spectrum is characteristic of a C_1-symmetrical species in which the helicoidal inversion has become very slow. The inversion barrier was calculated for protons H_γ at their coalescence temperature (302 K): $\Delta G^{\neq} = (59.7 \pm 0.5)\ kJ\,mol^{-1}$. The inversion barrier is the same as for $[ZnM_{(C_4)NH_2}]^{2+}$ in the same solvent ($\Delta G^{\neq} = (59.3 \pm 0.5)\ kJ\,mol^{-1}$). Although we have observed that the inversion barrier of the helicoidal equilibrium is sensitive to the length of the spacer, there is little impact of the nature of the coordinating group.

Monoclick reactions with other alcohol substrates: As in the case of the amines, the spacer can be slightly modified. Other alcohols such as 3-ethynylbenzyl alcohol ($ArCH_2OH$) and 4-pentyn-1-ol ($(C_3)OH$) allow a change in the spacer (Figure 9). Acetylene can also be substituted by a 4-nitrophenyl group, for example, pNO_2ArC_4OH. The monoclick reaction was conducted under the same conditions (10 equiv of 4-pentyn-1-ol or 3-ethynylbenzyl alcohol at reflux in dry toluene for 4 h). In both cases, the major product was the monofunctionalized product, but the precursor complex and the difunctionalized product were also usually observed. After purification by column chromatography and recomplexation with $Zn(ClO_4)_2{\cdot}(H_2O)_6$, the corresponding monofunctionalized complexes $[ZnM_{(C_3)OH}]^{2+}$ and $[ZnM_{ArCH_2OH}]^{2+}$ were obtained in good yields of 75–95%. Both complexes were characterized by EIMS ($m/z = 1498.6$ for $[ZnM_{(C_3)OH} + ClO_4]^+$ and $m/z = 1546.6$ for $[ZnM_{ArCH_2OH} + ClO_4]^+$). In contrast to $[ZnM_{(C_4)OH}]^{2+}$, the ^1H NMR spectra of $[ZnM_{(C_3)OH}]^{2+}$ and $[ZnM_{ArCH_2OH}]^{2+}$ in CD_3CN evidence only one C_s-symmetrical species with the pendant hydroxy chain out of the cavity and an acetonitrile molecule coordinated to the Zn^{II} ion. No self-coordinated complexes were observed.

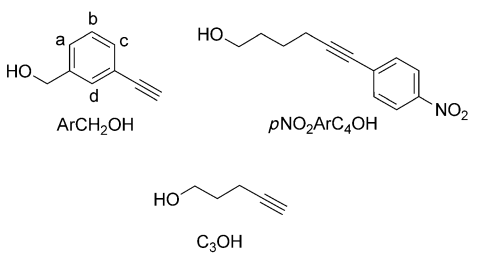

Figure 9. Hydroxy-acetylenes bearing different spacers and functionalities.

The reaction conducted with pNO_2ArC_4OH was much cleaner and much more selective. Indeed, the pure monofunctionalized complex $[ZnM_{pNO_2Ar(C)_4OH}]^{2+}$ was easily isolated after precipitation. It was characterized by EIMS ($m/z = 1633.6$ for $[ZnM_{pNO_2ArC_4OH} + ClO_4]^+$). Its ^1H NMR spectrum in CD_3CN at 300 K evidences a 75:25 mixture of the *exo* and *endo* complexes. VT NMR experiments in CD_3CN in the range 270–325 K gave the following thermodynamic parameters for the *endo*/*exo* equilibrium: $\Delta_r H^\circ = 3.8\ kJ\,mol^{-1}$ and $\Delta_r S^\circ = 22\ J\,K^{-1}\,mol^{-1}$. Compared with $[ZnM_{(C_4)OH}]^{2+}$, the self-coordination is enthalpically less favored, likely caused by the steric hindrance exerted by the *p*-nitrophenyl group at the large rim. The change in entropy is also much less positive, which can hypothetically be explained by the reduced mobility of the alkyl chain in the vicinity of the *p*-nitrophenyl group. These results evidence a stronger self-coordination effect with the *p*-nitrophenyl group compared with other alcohols, which diminishes the possibility of the displacement of the self-coordinated hydroxy chain in $[ZnM_{pNO_2Ar(C)_4OH}]^{2+}$ by a second pNO_2ArC_4OH molecule and thus rationalizes the better selectivity of the monoclick reaction. In CD_3CN, both the coordinated acetonitrile molecule and the self-coordinated hydroxy chain were classically displaced by the addition of one equivalent of propylamine to yield quantitatively the inclusion complex $[ZnM_{pNO_2ArC_4OH}(PrNH_2)]^{2+}$.

Conclusion

Selective functionalization of a macrocyclic structure presenting multiple and equally reactive sites is a real synthetic challenge. It generally represents a limiting step for appending valuable and spatially well-defined functions. In this paper we have presented a strategy based on host–guest chemistry that allows for the selective reaction of one out of three equivalent units of a calix[6]arene core. The strategy was inspired by natural systems, that is, enzymes that are well known to perform highly selective reactions under very mild conditions. The key points for enzymatic transformations are the formation of an enzyme–substrate complex and preorganization of the reactive partners (reactant/substrate) in the active-site pocket, which lead to low activation energy and high selectivity. The reaction implemented here is the thermal Huisgen cycloaddition, which, when noncatalyzed, requires high temperatures and leads to low regioselectivities. To take advantage of the host properties of the

calix[6]arene-based Zn^{II} funnel complexes, three azido groups were introduced at the large rim of the cavity (the reactant) and a coordinating moiety was appended to the alkyne substrates through a spacer (substrate). To explore the potentialities of this supramolecular strategy, four parameters were varied: 1) The nature of the coordinating moiety (primary amine vs. alcohol), 2) the length of the spacer from $(CH_2)_3$ to $(CH_2)_5$, 3) the shape of the spacer (linear alkane vs. phenyl nucleus), and 4) the substituent at the terminal site of the alkyne substrate.

Detailed structural and kinetic studies have evidenced interesting biomimetic features. The better the guest, the higher the reaction rate, which is related to thermodynamics through the host–guest binding constant *K*. The less sterically constrained the product, the higher the rate constant, which proves that embedment also has a significant impact on the transition state.

The high sensitivity of the system is nicely illustrated by the fact that a change of only one methylene group in the spacer length has a significant impact. The optimal C_4 length allows both a better preorganization and a lower-energy transition state in comparison with C_3 and C_5. Nevertheless, the flexibility of the host makes possible the efficient embedment of either a linear alkyl chain or a cyclic moiety. The efficiency of the confined reaction also permits alkynes bearing a sterically encumbered aromatic substituent at their terminal position to be grafted. All these results show that such a pre-association mimicking the Michaelis–Menten enzyme–substrate complex allows for the selective orientation of reactant versus substrate and a good pre-organization leading to lower activation energies. This is illustrated by the remarkably mild conditions under which this thermal Huisgen reaction proceeds compared with classical bimolecular reactions and also by the remarkable regioselectivity of the cycloaddition.

Finally, it is important to note that another key point of this synthetic strategy is the self-inhibition of the process. After covalent capture of a single guest, the intramolecular coordination link lowers the affinity of the metal center for exogenous ligands. With very good donors such as amines, the *endo* coordination is very strong and quasi-quantitative yields of monofunctionalized product are obtained. With the weaker donor alcohols, the transformation is less selective because the formation of around 5–10% of dialkylated products was observed. This is attributable to the more labile alcohol–Zn^{II} link that leads to more facile competition for the *endo* binding of a second equivalent of guest alcohol. Interestingly, the study related to such *endo–exo* competitive binding revealed that the self-coordination process of the appended alcohol function can be switched on and off by the presence of a more or less competing ligand. The equilibrium is shifted towards the *endo* adduct in pure $CDCl_3$ whereas the *exo* situation is obtained in the presence of one equivalent of a primary amine. The "ouroboros-like" behavior of this system actually offers the possibility of controlling the access to the cavity by using different kinds of stimuli. In this context, the use of an electrochemical input tuning the redox state of a copper ion is under investigation in our laboratory.

In conclusion, an in-depth analysis of the main factors governing the selectivity and efficiency of the supramolecular covalent capture process has shown that such a strategy is quite versatile and should be applicable to other cavitands associated with other recognition patterns. Also, this strategy could possibly be extended to other covalent capture reactions. Interestingly, such a covalent capture strategy has been recently applied to the synthesis of a carbonic anhydrase II mutant.[23]

Experimental Section

General procedure for the monoclick reaction with amines: Precursor complex $[ZnX_6N_3](ClO_4)_2$ (200 mg, 0.13 mmol, 1.0 equiv) was added to a solution of the appropriate amine (2 to 3 equiv) in dry toluene (10 mL). The resulting mixture was heated at reflux under argon for 2 h (for $(C_3)NH_2$ and $(C_4)NH_2$) and 5 h (for $(C_5)NH_2$). Toluene was evaporated under reduced pressure and the residue was redissolved in a minimum volume of acetonitrile (ca. 3 mL). The calixarene was then precipitated with diethyl ether (30 mL). The solid was filtered off, washed with diethyl ether (3×10 mL), and dried under vacuum.

General procedure for the monoclick reaction with alcohols: Precursor complex $[ZnX_6N_3](ClO_4)_2$ (200 mg, 0.13 mmol, 1.0 equiv) was added to a solution of the appropriate alcohol (10 equiv) in dry toluene (10 mL). The resulting mixture was heated at reflux under argon for 4 h. Toluene was evaporated under reduced pressure and the residue was redissolved in a minimum volume of acetonitrile (ca. 3 mL). The calixarene was then precipitated with diethyl ether (30 mL). The solid was filtered off, washed with diethyl ether (3×10 mL), and dried under vacuum. In the case of 6-(4-nitrophenyl)-5-hexyn-1-ol, the pure monofunctionalized complex was obtained without further purification. In the case of 5-hexyn-1-ol, 4-pentyn-1-ol, and 3-ethynylbenzyl alcohol, the crude product was purified by column chromatography on basic alumina ($CH_2Cl_2/CH_3OH/NH_3$ (27%), 99:1:0.01) to obtain the pure monofunctionalized calixarene ligand. The monofunctionalized ligand (20 mg, 1.0 equiv) was dissolved in a 1:1 mixture of CH_2Cl_2 and CH_3CN (1 mL). A solution of zinc perchlorate hexahydrate (1.0 equiv) predissolved in a minimum amount of THF was added to a solution of the ligand. After stirring for 15 min, diethyl ether was added (10 mL). The resulting precipitate was filtered off and dried under vacuum to provide the corresponding Zn^{II} complex as a white solid in 94–98% yield.

Full characterization data for all the monoclick products are presented in the Supporting Information.

Acknowledgements

This project was supported by the CNRS (Institut de Chimie), the Ministère de l'Enseignement Supérieur et de la Recherche, and the Agence Nationale pour la Recherche (Cavity-zyme(Cu) Project ANR-2010-BLAN-7141).

[1] a) M. B. Baker, I. Ghiviriga, R. K. Castellano, *Chem. Sci.* 2012, DOI: 10.1039/c2sc00943a; b) M. Lehmann, *Chem. Eur. J.* **2009**, *15*, 3638–3651; c) M. Lehmann, M. Jahr, *Chem. Mater.* **2008**, *20*, 5453–5456; d) D. G. Rivera, L. A. Wessjohann, *J. Am. Chem. Soc.* **2009**, *131*, 3721–3732; e) P. Gamez, J. Reedijk, *Eur. J. Inorg. Chem.* **2006**, 29–42.

[2] a) C. Ornelas, R. Pennell, L. F. Liebes, M. Weck, *Org. Lett.* **2011**, *13*, 976–979; b) L. Röglin, E. H. M. Lempens, E. W. Meijer, *Angew.*

Chem. **2011**, *123*, 106–117; *Angew. Chem. Int. Ed.* **2011**, *50*, 102–112; c) K. Sivanandan, B. S. Sandanaraj, S. Thayumanavan, *J. Org. Chem.* **2004**, *69*, 2937–2944; d) L. J. Prins, F. Mancin, P. Scrimin, *Curr. Org. Chem.* **2009**, *13*, 1050–1064; e) H. B. Albada, R. M. J. Liskamp, *J. Comb. Chem.* **2008**, *10*, 814–824; f) A. P. Davis, *Molecules* **2007**, *12*, 2106–2122; g) A. Gea, N. Farcy, N. Roqué i Rossell, J. C. Martins, P. J. De Clercq, A. Madder, *Eur. J. Org. Chem.* **2006**, 4135–4146; h) G. J. Rowlands, *Tetrahedron* **2001**, *57*, 1865–1882; i) M. J. W. Ludden, D. N. Reinhoudt, J. Huskens, *Chem. Soc. Rev.* **2006**, *35*, 1122–1134; j) L. Baldini, A. Casnati, F. Sansone, R. Ungaro, *Chem. Soc. Rev.* **2007**, *36*, 254–266; k) J. D. Badjić, A. Nelson, S. J. Cantrill, W. B. Turnbull, J. F. Stoddart, *Acc. Chem. Res.* **2005**, *38*, 723–732.

[3] P. Timmerman, W. Verboom, D. N. Reinhoudt, *Tetrahedron* **1996**, *52*, 2663–2704.

[4] J. Lagona, P. Mukhopadhyay, S. Chakrabarti, L. Isaacs, *Angew. Chem.* **2005**, *117*, 4922–4949; *Angew. Chem. Int. Ed.* **2005**, *44*, 4844–4870.

[5] J. Szejtli, *Chem. Rev.* **1998**, *98*, 1743–1753.

[6] a) C. D. Gutsche, in *Calixarenes An introduction*, Monographs in: Supramolecular Chemistry, (Ed: J. F. Stoddart, The Royal Society of Chemistry, Cambridge), 2nd ed., **2008**; b) C. D. Gutsche, in *Calixarenes Revisited*, Monographs in: Supramolecular Chemistry, (Ed: J. F. Stoddart, The Royal Society of Chemistry, Cambridge), **1998**.

[7] a) K. Teranishi, *Chem. Commun.* **2000**, 1255–1256; b) K. Teranishi, *Tetrahedron* **2003**, *59*, 2519–2538; c) K. Teranishi, *J. Inclusion Phenom. Macrocyclic Chem.* **2002**, *44*, 313–316; d) D. Rong, T. D'Souza, *Tetrahedron Lett.* **1990**, *31*, 4275–4278; e) H. Cousin, P. Cardinael, H. Oulyadi, X. Pannecoucke, J. C. Combret, *Tetrahedron: Asymmetry* **2001**, *12*, 81–88; f) P. Fügedi, P. Nánási, *Carbohydr. Res.* **1988**, *175*, 173–118; g) Z. Chen, J. S. Bradshaw, M. L. Lee, *Tetrahedron Lett.* **1996**, *37*, 6831–6834; h) A. R. Khan, P. Forgo, K. J. Stein, V. T. D'Souza, *Chem. Rev.* **1998**, *98*, 1977–1996.

[8] R. F. Gómez-Biagi, M. Nitz, *Chem. Commun.* **2011**, *47*, 8614–8616.

[9] a) M. Ahmed, K. Koga, M. Fukudome, H. Sasaki, D. Yuan, *Tetrahedron Lett.* **2011**, *52*, 4646–4649; b) D. Lucas, T. Minami, G. Iannuzzi, L. Cao, J. Wittenberg, P. Anzenbacher, L. Isaacs, *J. Am. Chem. Soc.* **2011**, *133*, 17966–17976; c) N. Zhao, G. O. Lloyd, O. A. Scherman, *Chem. Commun.* **2012**, *48*, 3070–3072.

[10] a) A. R. Renslo, J. Rebek Jr., *Angew. Chem.* **2000**, *112*, 3419–3421; *Angew. Chem. Int. Ed.* **2000**, *39*, 3281–3283; b) U. Lücking, F. C. Tucci, D. M. Rudkevich, J. Rebek Jr., *J. Am. Chem. Soc.* **2000**, *122*, 8880–8889; A. R. Renslo, D. M. Rudkevich, J. Rebek Jr., *J. Am. Chem. Soc.* **1999**, *121*, 7459–7460; c) A. R. Renslo, F. C. Tucci, D. M. Rudkevich, J. Rebek Jr., *J. Am. Chem. Soc.* **2000**, *122*, 4573–4582; d) U. Lücking, D. M. Rudkevich, J. Rebek Jr., *Tetrahedron Lett.* **2000**, *41*, 9547–9551; e) S. D. Starnes, D. M. Rudkevich, J. Rebek Jr., *Org. Lett.* **2000**, *2*, 1995–1998; f) S. D. Starnes, D. M. Rudkevich, J. Rebek Jr., *J. Am. Chem. Soc.* **2001**, *123*, 4659–4669; g) S. Richeter, J. Rebek Jr., *J. Am. Chem. Soc.* **2004**, *126*, 16280–16281; h) A. Gissot, J. Rebek Jr., *J. Am. Chem. Soc.* **2004**, *126*, 7424–7425.

[11] B. Colasson, O. Reinaud, *J. Am. Chem. Soc.* **2008**, *130*, 15226–15227.

[12] R. Huisgen, *Angew. Chem.* **1963**, *75*, 604–637; *Angew. Chem. Int. Ed. Engl.* **1963**, *2*, 565–598.

[13] a) O. Sénèque, M.-N. Rager, M. Giorgi, O. Reinaud, *J. Am. Chem. Soc.* **2000**, *122*, 6183–6189; b) D. Coquière, S. Le Gac, U. Darbost, O. Sénèque, I. Jabin, O. Reinaud, *Org. Biomol. Chem.* **2009**, *7*, 2485–2500.

[14] M represents the monofunctionalized calix[6]arene, C_3 indicates that a three methylene chain connects the amino and acetylene groups, and NH_2 indicates that the coordinating unit is an amino group. The descriptor M_{C_nX} is used throughout the manuscript.

[15] In the absence of Zn^{II}, the reaction does not show any conversion. The addition of a Cu^{I} catalyst leads to a mixture of triazole products.

[16] Ouroboros ("tail-eater" in Greek) is an ancient symbol representing a serpent swallowing its own tail, see: a) F. Durola, J. Rebek Jr., *Angew. Chem.* **2010**, *122*, 3257–3259; *Angew. Chem. Int. Ed.* **2010**, *49*, 3189–3191; b) S. Nygaard, Y. Liu, P. C. Stein, A. H. Flood, J. O. Jeppesen, *Adv. Funct. Mater.* **2007**, *17*, 751–762; c) Y. Enmi, K. Kobayashi, H. Konishi, M. Morimoto, *Tetrahedron Lett.* **2011**, *52*, 3367–3370.

[17] We assume that the calculated ratio of equilibrium constants remains valid under the reaction conditions (toluene, 110 °C) because the structures of the three amines are very similar and no solvent effects are expected to favor the complexation of one particular guest.

[18] K. Kano, M. Kondo, H. Inoue, H. Kitagishi, B. Colasson, O. Reinaud, *Inorg. Chem.* **2011**, *50*, 6353–6360.

[19] At room temperature, the exchange of two amine guests in the receptor takes place within less than a minute. At 110 °C, the timescale for the cycloaddition reaction is around 2 h.

[20] B. Colasson, M. Save, P. Milko, J. Roithová, D. Schröder, O. Reinaud, *Org. Lett.* **2007**, *9*, 4987–4990.

[21] a) O. Sénèque, Y. Rondelez, L. Le Clainche, C. Inisan, M.-N. Rager, M. Giorgi, O. Reinaud, *Eur. J. Inorg. Chem.* **2001**, 2597–2604; b) O. Sénèque, M. Giorgi, O. Reinaud, *Supramol. Chem.* **2003**, *15*, 573–580.

[22] Because the reactions with the two substrates *p*$NO_2Ar(C_4)NH_2$ and *p*$OMeAr(C_4)NH_2$ need 5 h to go to completion, we privilege steric rather than electronic factors for the discussion about the reaction rates.

[23] J. S. Wischeler, D. Sun, N. U. Sandner, U. Linne, A. Heine, U. Koert, G. Klebe, *Chem. Eur. J.* **2011**, *17*, 5842–5851.

Received: July 5, 2012
Revised: September 24, 2012
Published online: November 20, 2012

